Design and performance test of a novel UAV air-assisted electrostatic centrifugal spraying system

Heming Hu[1], Yutaka Kaizu[1], Jingjing Huang[2,4], Kenichi Furuhashi[1], Hongduo Zhang[1], Xu Xiao[3], Ming Li[2,3*], Kenji Imou[1*]

(1. *Graduate School of Agricultural and Life Sciences, the University of Tokyo, Tokyo 113-0033, Japan*;
2. *Hunan Agricultural Equipment Research Institute, Changsha 410125, China*;
3. *Hunan Advanced Engineering Technology Research Center for Agricultural Aviation, Changsha 410125, China*;
4. *Hunan Agricultural University, Changsha 410128, China*)

Abstract: In order to improve the deposition and uniformity of the pesticide sprayed by the agricultural spraying drone, this study designed a novel spraying system, combining air-assisted spraying system with electrostatic technology. First, an air-assisted electrostatic centrifugal spray system was designed for agricultural spraying drones, including a shell, a diversion shell, and an electrostatic ring. Then, experiments were conducted to optimize the setting of the main parameters that affect the charge-to-mass ratio, and outdoor spraying experiments were carried out on the spraying effect of the air-assisted electrostatic centrifugal spray system. The results showed the optimum parameters were that the centrifugal rotation speed was 10 000 r/min, the spray pressure was 0.3 MPa, the fan rotation speed was 14 000 r/min, and the electrostatic generator voltage was 9 kV; The optimum charge-to-mass ratio of the spray system was 2.59 mC/kg. The average deposition density of droplets on the collecting platform was 366.1 particles/cm^2 on the upper layer, 345.1 particles/cm^2 on the middle layer, and 322.5 particles/cm^2 on the lower layer. Compared to the results of uncharged droplets on the upper, middle, and lower layers, the average deposition density was increased by 34.9%, 30.4%, and 30.2%, respectively, and the uniformity of the distribution of the droplets at different collection points was better.

Keywords: UAV spraying, droplet drift, centrifugal sprayer, air-assisted spraying, electrostatic spraying
DOI: 10.25165/j.ijabe.20221505.6891

Citation: Hu H M, Kaizu Y, Huang J J, Furuhashi K, Zhang H D, Xiao X, et al. Design and performance test of a novel UAV air-assisted electrostatic centrifugal spraying system. Int J Agric & Biol Eng, 2022; 15(5): 34–40.

1 Introduction

Compared with hydraulic nozzles, centrifugal sprayers can atomize droplets evenly. However, since the centrifugal sprayers spray droplets in the horizontal direction, the droplets are more likely to drift[1-4]. Electrostatic spray technology, which decreases droplet drift and increases droplet deposition and penetration[5-10], are widely used in the agricultural spraying system on unmanned aerial vehicle (UAV). Air-assisted spray technology, using a fan to produce stable downward wind to increase the initial velocity of the droplets[11,12], will effectively improve the insufficient deposition of the centrifugal nozzle.

The aerial electrostatic spray technology had a history of more than half a century, and many studies have been carried out[13-16]. Inculet et al.[17] designed the coplanar charging of oppositely charged droplet clouds to reduce the accumulation of charge on a plane, which marked the rapid development of the aerial electrostatic spray system.

An indicator to measure the quality of electrostatic spray is the charge-to-mass ratio, normally the greater the charge-to-mass ratio, the better the deposition effect[18]. Lan et al.[19] proposed that droplets were found to be easily charged when droplet diameter is below 120 μm, and under the charging voltage of 8 kV, the spray system had the best charge-to-mass ratio, of 0.22 mC/kg. Maski et al.[20,21] investigated the deposition of charged spray on the back and surface of the blade as influenced by the spray charging voltage, target height, and direction. They proposed that the performance combination of electrode voltage and liquid flow rate could improve the chargeability of electrostatic sprays. Zhang et al.[22] designed a UAV airflow electrostatic atomization device, and the test result showed a better deposition density on the upper, middle, and lower layers of rice crops.

Previously, researchers mainly focused on the hydraulic nozzle electrostatic spraying system, including the influence of electrode material, charging voltage, and charging method on the deposition density of the spray system. Centrifugal sprayers can spray pesticides more uniformly within the operating radius, but electrostatic spray systems based on centrifugal sprayers have not been studied deeply.

Received date: 2021-07-13 **Accepted date:** 2022-06-14
Biographies: Heming Hu, PhD candidate, research interest: agricultural aerial spraying, image processing, Email: hu-heming950211@g.ecc.u-tokyo.ac.jp; **Yutaka Kaizu**, PhD, Associate Professor, research interest: machine vision, 3D mapping, field robotics, navigation, GPS, Email: kaizu@g.ecc.u-tokyo.ac.jp; **Jingjing Huang**, MS, research interest: agricultural intelligent equipment, Email: huangjingjing2016@gmail.com; **Kenichi Furuhashi**, PhD, Assistant Professor, research interest: biomass energy Email: kfuruhashi@g.ecc.u-tokyo.ac.jp; **Hongduo Zhang**, PhD candidate, research interest: agricultural robot, Email: zhdhnhr@outlook.com; **Xu Xiao**, PhD candidate, research interest: agricultural robot, Email: 395949410@qq.com;

***Corresponding author: Ming Li**, PhD, Professor, research interest: crops sensing information acquisition and agricultural robots. Hunan Agricultural Equipment Research Institute, No.480, Donghu Road, Furong District, Changsha 410125, China. Tel: +86-15974170086, Email: liming@hunau.net; **Kenji Imou**, Professor, PhD, Professor, research interest: renewable energy, bio fuel, Navigation sensor, autonomous vehicle, image processing. The University of Tokyo, Graduate School of Agricultural and Life Sciences, 1-1-1, Yayoi, Bunkyo-ku, Tokyo, 113-8657, Japan. Email: k-imou@g.ecc.u-tokyo.ac.jp.

Currently, centrifugal spraying technology atomizes pesticides mainly by centrifugal motion of centrifugal turntable[23,24]. Centrifugal atomization technology was one of the most suitable methods to obtain uniform fine droplets and also to adjust the droplet size in a wide range. Craig et al.[25] added sharp ejection points or needles to existing centrifugal nozzle designs, dramatically improved the efficiency of pesticide application to aircraft, and reduced the downwind buffer distance on avoiding drift damage and droplet drift. Derksen et al.[26] proposed that pest and disease problems occurred in specific locations on plants and used air-assisted methods to increase the penetration of pesticide sprays. Bayat et al.[27] combined centrifugal nozzle and air-assisted system to investigate its effect on spray penetration, deposition, and drift reduction, the combination largely increased the speed and droplet diameter. Meanwhile, downwind drift was partially controlled at an air-assisted velocity of 25 m/s, when the drift potential could be reduced to 39%.

In sum, previous studies mainly focused on hydraulic nozzles. However, centrifugal sprayers were not easy to block and have a larger spray radius adjustment range compared to hydraulic nozzles. Therefore, the centrifugal nozzle was selected as the research object since the centrifugal nozzle ejects droplets horizontally, the droplets have no initial downward velocity and were prone to drift, to make the deposition and uniformity of the centrifugal sprayer better, this study combines electrostatic spraying and air-assistant technology to improve the spraying performances of the centrifugal nozzle.

2 Materials and methods

2.1 UAV parameter

As shown in Figure 1, the UAV used in the study was 3WX6-10, which was produced by Hunan soar-star aviation technology Co., Ltd. The UAV featured large load capability and long endurance, which has a maximum battery duration of 28 min with a maximum load of 16 kg. The UAV is equipped with carbon fiber base with aluminum alloy arms, making it light weight and strong. Its main properties are listed in Table 1.

Figure 1 3WX6-10 UAV

Table 1 Main performance parameters of 3WX6-10 UAV

Parameters	Value
Max load/kg	16
Max flight speed/m·s^{-1}	7
UAV (no battery) mass/kg	18.5
Paddle size/m	10.0×2.8
Dimensions (L×W×H)/(mm×mm×mm)	2520×2212×720
Number of rotors	6
Max endurance (no load)/min	28
Pesticide box volume/L	10
Operational efficiency/m^2·h^{-1}	24 000

2.2 Air supply system

A high-flow, high-thrust electric duct fan produced by FMS-model Co. Ltd., China is shown in Figure 2. The fan is able to output a maximum of 900 grams of thrust when the rotor speed reaches 20 000 r/min.

Figure 2 64 mm 11-blade duct fan

Solidworks software was used to design the air supply cylinder as shown in Figure 3.

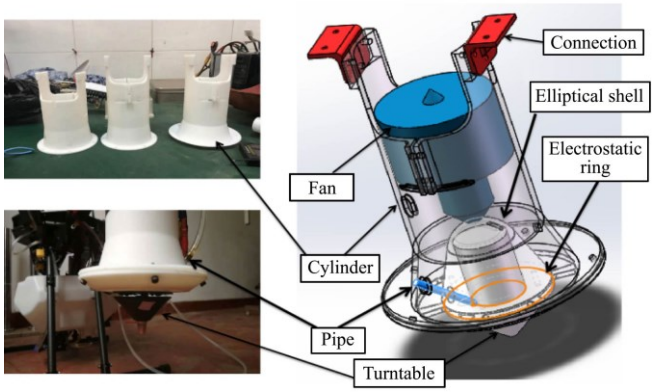

Figure 3 Air-assisted electrostatic centrifugal spraying system

The diameter and height of this spray system are 130 mm and 210 mm, respectively. The entire spray system was composed of fan, cylinder, pipe, electrostatic ring, elliptical shell, and connection. The entire system was powered by a single 3S battery and the total power is 1200 W. The function of the air supply cylinder was to fix the fan and centrifugal turntable under drone's wings, and to guide the air conveyed by the fan. The upper connections were able to fix the cylinder under the UAV. The elliptical shell located below the fan can significantly accelerate the air outflow. To avoid droplets hitting the surface of the air supply cylinder, the end of air supply cylinder was designed to curve outward. This design will effectively avoid the waste of pesticides (droplets collision on the cylinder) and accelerate the outflow of air. An electrostatic ring is placed between the turntable and the elliptical deflector shell for charging the droplet.

2.3 Electrostatic spray system

2.3.1 Principle of electrostatic spray

For centrifugal spray systems, there were three ways to charge pesticide, namely induction charging, corona charging, and contact charging as shown in Figure 4. Comparing the three ways, it is concluded that contact charging and corona charging need more than 20 kV, while induction charging voltage is less than 10 kV, which can save battery power supply and pose a safety hazard.

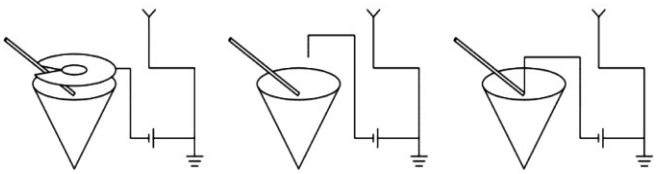

a. Induction charging b. Corona charging c. Contact charging

Figure 4 Charging method of electrostatic spraying

Figure 5 shows an equivalent circuit of induction charging. As for induction charging, the electrostatic generator was connected to the electrostatic generating ring placed in the air

supply cylinder. The air between the ring electrode and the liquid was considered an insulator, which was the capacitance *C*, and its resistance is R1.

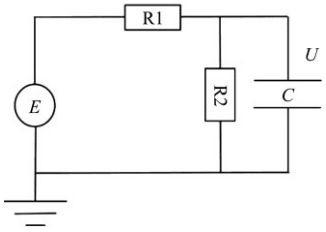

Figure 5 Equivalent electrical circuit diagram of induction charging

The electric potential of electrostatic generating ring is the charging voltage *U*. The potential of the electrostatic generator is *E*, and the internal resistance of the generating ring is R2.

2.3.2 Design of the electrostatic spray system

The electrostatic generator, produced by Yufei Technology Co., Ltd., is shown in Figure 6, of which the length is 112 mm, the input power is less than 5 W, and the adjustable output voltage is from 5 to 20 kV.

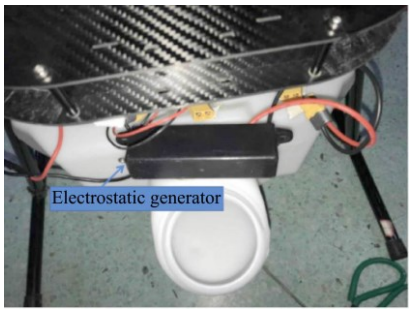

Figure 6 Electrostatic generator

The high-voltage electrostatic generator was directly connected to the charging electrode to provide high voltage so that the electrostatic field is generated inside the electrode, as shown in Figure 7. The electrostatic field changes the charge distribution in the water stream, and when the water stream is broken, the droplets were charged.

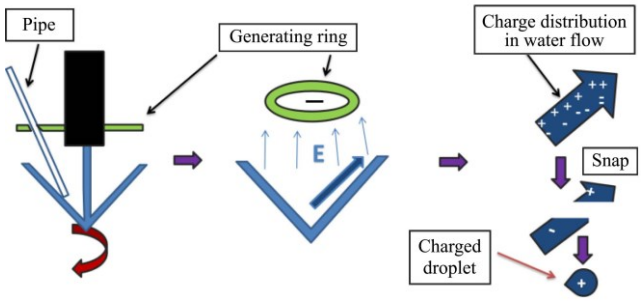

Figure 7 Working principle of electrostatic centrifugal spray

Under the action of electric field force and gravity and wind, the droplets moved to crops. As the droplet approaches the surface of the crop, the electrostatic induction made the crop surface with the opposite charge of the droplet, then the liquid deposited on the crop surface evenly.

From the principle of induction charging, the charged amount of the induction generating ring can be calculated by Equation (1).

$$Q = C \times U \tag{1}$$

where, Q is the amount of charge carried by the inductively charged ring; C is the capacitance of the capacitor; U is the voltage of the electrostatic generator. The capacitance is calculated by Equation (2).

$$C = \frac{\varepsilon S}{4\pi k d} \tag{2}$$

where, ε is the value of the dielectric constant between the electrostatic generating ring and the liquid; S is the cross-sectional area of the electrostatic generating ring; k is the electrostatic force constant; d is the distance between the electrode and the liquid film. Equations (1) and (2) show that the main factors affecting the amount of droplet charge are the charging voltage U, and the distance between the electrode and the liquid d. The design of the electrostatic ring is shown in Figure 8.

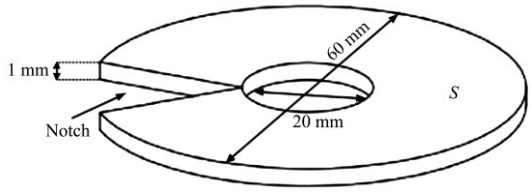

Figure 8 Electrostatic generating ring

The electrostatic generating ring was made by cutting stainless steel. The diameter of the electrostatic generating ring is consistent with the outer diameter of the centrifugal turntable. The thickness is 1 mm, and the notch is designed to facilitate water into the water inlet.

According to Equation (3)[29], the electric field intensity is concentrated on the vertical plane, so the electrostatic ring is placed horizontally above the turntable. Here, θ=0 or π, r can be replaced with Z, which can calculate Equation (4).

$$d\vec{L} - \frac{}{4\pi\varepsilon R^3} = \frac{}{4\pi\varepsilon(\alpha^2 + r^2 - 2ar\sin\theta\cos\theta)^{\frac{3}{2}}} \tag{3}$$

$$E_x = 0,\ E_y = 0,\ E_z = \frac{\pm\eta\alpha z}{2\varepsilon(\alpha^2 + z^2)^{\frac{3}{2}}} \tag{4}$$

where, E is the field strength in the direction. It is known that the area where the droplets form is on the edge of the centrifugal turntable, so r is the linear distance from the edge of the centrifugal turntable to the induced electrostatic generation ring. α is the inner diameter of the induction ring. According to Equation (4), $r/\alpha = \sqrt{2}/2$. Because the motor needs to be connected above the centrifugal turntable, the inner diameter of the induction motor was set to be slightly larger than the motor diameter, which is 20 mm. Therefore, in order to achieve the best charging effect, the height of the electrostatic generation ring was set to be 14 mm from the highest plane of the centrifugal turntable.

2.4 Methods

2.4.1 Fan's effective working range

The effect of the fan on the spray radius was conducted to find out its effective working range.

As shown in Figure 9, the spray system was placed 60 cm above the inclined V-grooves with 10 cm intervals and 150 cm long. At the bottom of the V-grooves, 17 cups were set up to collect the sprayed droplets, and the spray system was placed above the No. 9 cup in the middle. Then spray system was turned on for 20 s, and the sprayed droplets hit the V-grooves and flowed into the measuring cups. After spraying, the weights of the measuring cups were measured with a balance. The distribution of droplets is obtained according to the distribution of the weights of the measuring cups. In order to obtain the effective working range of the fan, a single variable is adopted. First, the bottom turntable is set to the lowest limit of normal operation, and the rotation speed of the fan is gradually increased to study the change in droplet

distribution. Here we define that the effective working range of a fan is that the fan can significantly affect the distribution of droplets.

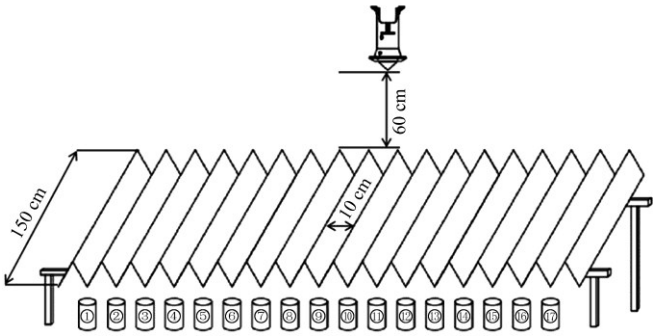

Note: 17 cups were set up to collect the sprayed droplets.

Figure 9 Test device of working radius

2.4.2 Parameters for suitable droplet size

From previous studies[19,30], it is clear that droplet size under 120 μm is not only easy to charge but also significantly increases the effectiveness of the droplets on pest control of crops. The three parameters of the spraying system that affect the droplet size were selected for this experiment, including spraying pressure, fan speed, and bottom turntable speed.

As shown in Table 2, spray pressure was selected as the level of the pump pressure factor within the rated working spray pressure of 0.25 MPa, 0.30 MPa, and 0.35 MPa. Centrifugal turntable speed level selected 6000 r/min, 8000 r/min, and 10 000 r/min as the three levels. According to the above fan effective working range test, the fan speed was selected as three levels: 14 000 r/min, 16 000 r/min, and 18 000 r/min. Nine sets of cross-tests were conducted for the three sets of parameters.

Table 2 Cross test design for optimal parameters determination

Test level	$N1$ Turntable speed/r·min^{-1}	P Pump pressure/MPa	$N2$ Fan speed/r·min^{-1}
1	6000	0.25	14 000
2	8000	0.30	16 000
3	10 000	0.35	18 000

Prior to the test, the fan and the bottom turntable speeds were adjusted according to the cross-test table. Then as shown in Figure 10, eight collection points were set up at 1 m intervals, and water-sensitive paper was glued to the droplet collection platform at 1 m above the surface of the field. The spray system was operated over the droplet collection points and left traces on the water-sensitive paper. Droplet images were obtained by scanning the water-sensitive paper. The droplet images were analyzed to obtain the droplet diameters by image-J software.

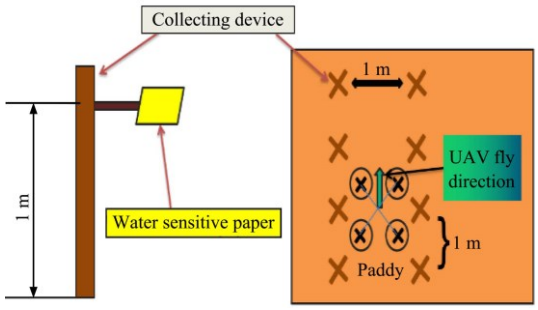

Figure 10 Droplet size collection test

The UAV took off and after aligning the flight path, the flight height was 2 m, and the pump pressure parameters were adjusted to the specified values for that group of tests. After completing the experiments, the water-sensitive paper collected was sealed and scanned.

2.4.3 Optimal charge-to-mass ratio parameter test

In test No. 6 parameters in the previous test group: turntable speed of 800 r/min, pump pressure of 0.35 MPa, and the fan speed of 14 000 r/min, No. 7 parameters: turntable speed of 10 000 r/min, pump pressure of 0.25 MPa, and the fan speed of 18 000 r/min, No. 8 parameters: the fan speed of 10 000 r/min, pump pressure of 0.30 MPa, and the fan speed of 14 000 r/min. The three groups of parameters were matched with five different electrostatic generators voltages of 6 kV, 7 kV, 8 kV, 9 kV, and 10 kV to compare the size of the spray charge-to-mass ratio produced under different static voltages in each parameter.

The equation for calculating the charge-to-mass ratio A_n (mC/kg) is,

$$A_n = \frac{Q}{m} = \frac{I \cdot t}{(G_2 - G_1)} \tag{5}$$

where, Q is the amount of charge, mC; I is the induced current intensity, mA; t is the measurement time, s; G_1 is the initial weight on the scale; G_2 is the end weight on the scale.

The magnitude of the charge-to-mass ratio was detected by the mesh target method, as shown in Figure 11 by wrapping a circle of insulating tape around the outside of the barrel to ensure that the charge inside the cylinder is not exchanged with the outside world. Barrel has two interfaces connected to the ground and the picoammeter respectively.

Figure 11 Barrel with wire mesh

As shown in Figure 12 the spray system was inserted into the insulating barrel, and when the sprayed droplets from the electrostatic spray system collided with the wire mesh inside the iron cylinder, they form a circuit with the ground and generated a microcurrent. The current I was measured with a picoammeter, Keithley 6485-A. The picoammeter has an average calculation function, which can directly read out the average value of the current in the corresponding time. At the same time, the initial and final masses G_1 and G_2 of the insulated cylinder per unit time t were measured with an electronic balance.

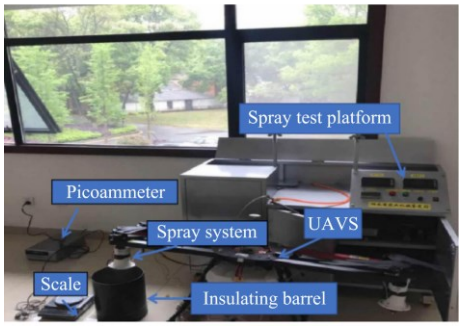

Figure 12 Devices of charge-to-mass test

2.4.4 Outdoor spray test

To test the efficiency of the air-assisted electrostatic centrifugal spray system, two control groups were set up with the electrostatic generator turned off and at different flight altitudes. The spray

distribution uniformity and droplet deposition density of the spray system were measured at positions as shown in Figure 13. Outdoor test procedures were compared under electrostatic and non-electrostatic conditions. The outdoor temperature was 25°C, the liquid in the tank was water, the amount of water carried was 5 L, and the flight speed was set to 3 m/s.

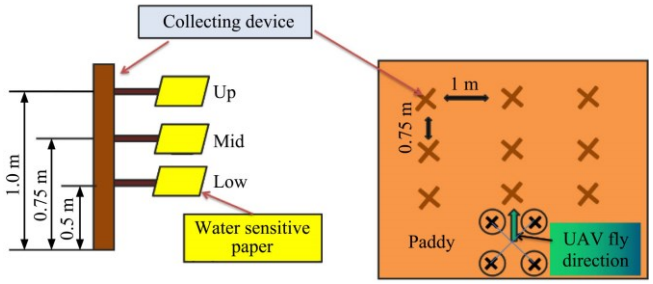

Figure 13 Outdoor test procedure

As shown in Figure 14, each droplet collection device was divided into three layers, the heights were 100 cm, 75 cm, and 50 cm. The outdoor experiments were set up in three groups of parameters: charged droplet at flight altitude 2 m, uncharged droplet at flight altitude 2 m, and uncharged droplet at flight altitude 3 m. In every case, the pump pressure was set to 0.3 MPa, the centrifugal turntable speed was set to 10 000 r/min, the fan speed was set to 14 000 r/min, and the voltage was set to 9 kV when the static electricity was turned on.

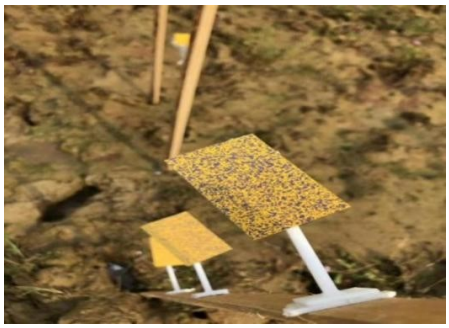

Figure 14 Field Test Collection Process

3 Results and discussion

3.1 Result of fan's effective working range

The droplet distribution under different fan r/min and turntable r/min was shown in Figure 15, the black bar graph represented the distribution of droplets under the parameters without fan and low turntable r/min, the distribution of droplets was not uniform, and according to observation the higher bar on the left side was the result of droplets hitting on the pesticide box.

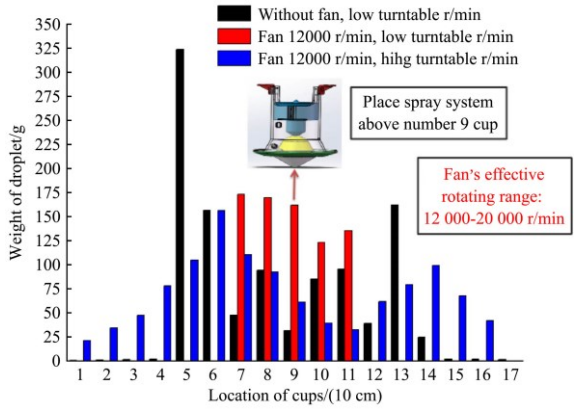

Figure 15 Bar graph of the droplets distribution

Keeping the turntable r/min unchanged, the fan speed was gradually increased until 12 000 r/min, here droplets did not hit the pesticide box. As is shown in red bar the distribution of droplets became uniform. Then, increased the speed of the turntable and kept the fan speed at 12 000 r/min, the distribution of droplets showed a normal distribution as the blue bars shown in the graph, also the droplets did not hit the tank. The upper-speed limit of the fan is 20 000 r/min, therefore the effective speed range of the fan of this spraying system is 12 000-20 000 r/min.

3.2 Result of suitable droplet size

According to the results listed in Table 3, at test numbers 6, 7, and 8, the resulting droplet sizes were less than 120 μm. These parameters were chosen for further experiments.

Table 3 Results of the droplet size

Test number	N1 Turntable speed /r·min^{-1}	P Pump pressure /MPa	N2 Fan speed /r·min^{-1}	Droplet size /μm
1	6000	0.25	14 000	253.1
2	6000	0.30	16 000	274.5
3	6000	0.35	18 000	159.9
4	8000	0.25	16 000	123.1
5	8000	0.30	18 000	134.3
6	8000	0.35	14 000	118.1
7	10 000	0.25	18 000	96.6
8	10 000	0.30	14 000	106.3
9	10 000	0.35	16 000	130.2

The influence of parameters on particle size was further analyzed. In Table 4, the numerical values of K1, K2, and K3 correspond to the rotation speed of the centrifugal turntable, spray pressure, and the rotation speed of the channel fan at levels 1, 2, and 3, respectively. R represents the range of K1, K2, and K3. It can be seen from Table 4 that the range of the rotational speed of the centrifugal turntable is the largest, so the rotational speed of the centrifugal turntable has the greatest influence on the particle size of the droplets, followed by the effect of the ducted fan on the particle size of the droplets, and the smallest influencing factor is the water pump pressure.

Table 4 Level test standard deviation range analysis

Standard deviation and range	N1 Turntable speed	P Pump pressure	N2 Fan speed
K1	687.5	472.8	477.5
K2	375.5	515.1	527.8
K3	333.1	408.2	390.8
R	354.4	106.9	137.0

3.3 Results of charge-to-mass ratio

The results are listed in Table 5. The experiment determined that when the centrifugal turntable speed was 10 000 r/min, the pump pressure was 0.3 MPa, the fan speed was 14 000 r/min, and the charging voltage was 9 kV, the average particle size of the sprayed droplets was 106.3 μm, and the sprayed droplets were charged with the highest charge-to-mass ratio of 2.59 mC/kg. Further analysis of the relationship between the charge-to-mass ratio and the electrostatic voltage, the increasing rate of the charge-to-mass ratio fluctuated, in the interval of 7-8 kV, and 8-9 kV, the charge-to-mass ratio changed greatly, but in the interval of 9-10 kV, the charge-to-mass ratio increased little. At the same time, the voltage of the maximum charge-to-mass ratio is not the maximum voltage of 10 kV given in the test, so it is inferred that the effect of induced charging reaches saturation near the voltage of 10 kV.

Table 5 Value of charge-to-mass ratio at different parameters

Test number	Charge-to-mass ratio/mC·kg^{-1}				
	6 kV	7 kV	8 kV	9 kV	10 kV
6	1.61	1.84	1.98	2.21	2.34
7	1.69	1.81	2.17	2.37	2.41
8	1.72	1.77	2.32	2.59	2.58

3.4 Result of droplet deposition and distribution

The average droplet deposition and deposition results for each collection device are shown in Table 6. At a flying height of 2 m, the average deposition densities of the charged droplets are 94.7 particles/cm^2, 80.5 particles/cm^2, 74.9 particles/cm^2 higher than the uncharged droplet, in the upper, middle, and lower part of the collecting device perspective.

Table 6 Deposition density results of three groups of tests (particle·cm^{-2})

Parameters positions	Upper average deposition density	Mid average deposition density	Lower average deposition density
Height 2 m Charged	366.1	345.1	322.5
Height 2 m Uncharged	271.4	264.6	247.6
Height 3 m Uncharged	270.1	234.7	215.5

Figure 16 showed the droplets deposition at different positions. By comparing the coefficient of variation, the charged droplet was 14.1%, 23.8%, and 31.9% in the upper, middle and low, compared to the uncharged droplet (2 m) 42.8%, 45.7%, 33.3%, charged droplets were more evenly distributed, their distribution of deposition density was more concentrated to average value in the figure.

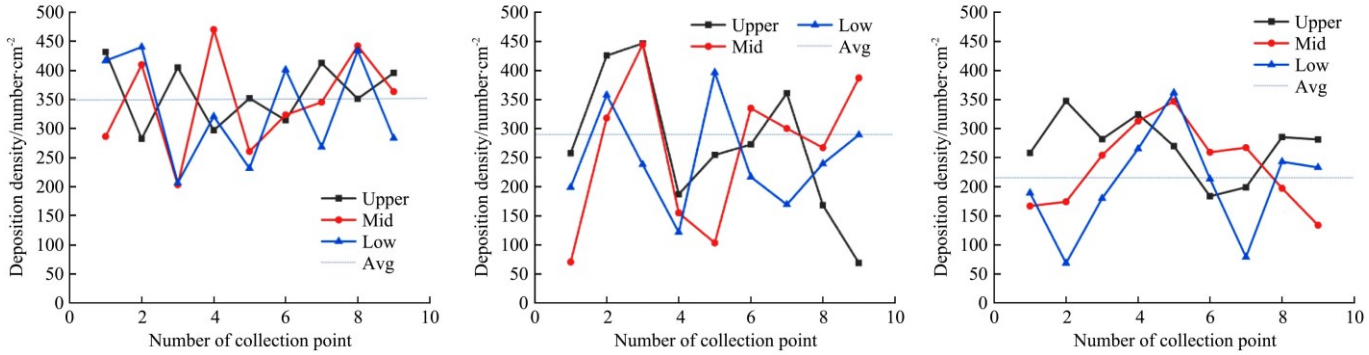

a. Charged droplet (at height of 2 m) b. Uncharged droplet (at height of 2 m) c. Uncharged droplet (at height of 3 m)

Figure 16 Distribution of droplets on collecting points

In the case of uncharged droplets at 3 m, the deposition did not become very poor compared to a height of 2 m, therefore the flying height is not an important factor affecting the deposition effect compared to electrostatic force in this spray system. As is shown in Figure 17, when electrostatic was involved, the droplets were thinner and more evenly distributed, typically the smaller the particle size of the droplets on the crop surface, the higher the surface area of the droplets per unit mass. Which helps reduce pesticide spraying and enables precise spraying.

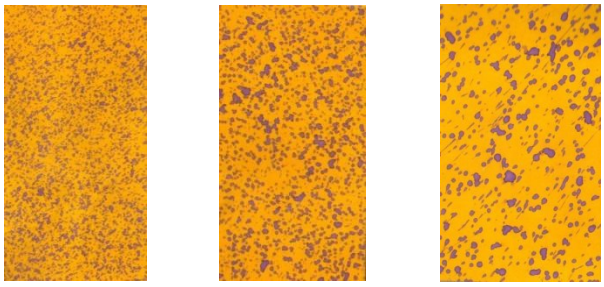

a. 2 m with electricity b. 2 m without electricity c. 3 m without electricity

Figure 17 Deposition Image of droplet on water sensitive paper

4 Conclusions

To reduce droplet drift and improve the uniformity of droplets, an air-driven centrifugal electrostatic spray system for plant protection UAV was designed in this study.

Through the optimal parameter tests, it was determined that when the centrifugal turntable rotation speed was 10 000 r/min, the spray pressure was 0.3 MPa, the fan speed was 14 000 r/min, and the charging voltage was 9 kV, the average particle size of the sprayed droplets was 106.3 μm. The droplet had the highest charge-to-mass ratio of 2.59 mC/kg.

Outdoor tests were conducted on the UAV electrostatic spray system under the optimal parameters, it was concluded that the air-driven centrifugal electrostatic spray system has a good effect on improving the penetration ability, uniformity of the droplets, and improving the deposition of the pesticide on the crop.

Acknowledgements

This work was financially supported by the National Key Research and Development Program of China (Grant No. 2018YFD0200800); the Key Research and Development Program of Hunan Province (Grant No. 2018GK2013); Hunan Modern Agricultural Industry Technology Program (Grant No. 201926); Innovation and Entrepreneurship Training Program of Hunan Agricultural University (Grant No. 2019062x).

[References]

[1] Ru Y, Jin L, Zhou H P, Jia Z C. Performance experiment of rotary hydraulic atomizing nozzle for aerial spraying application. Transactions of the CSAE, 2014; 30(3): 50–55. (in Chinese)

[2] Liu X, Zhang W, Fu H B, Fu X M, Qi L Q. Distribution regularity of downwash airflow under rotors of agricultural UAV for plant protection. Int J Agric & Biol Eng, 2021; 14(3): 46–57.

[3] Wang G B, Han Y X, Li X, Andaloro J, Chen P C, Hoffmann W C, et al. Field evaluation of spray drift and environmental impact using an agricultural unmanned aerial vehicle (UAV) sprayer. Science of the Total Environment, 2020; 737: 139793. doi: 10.1016/j.scitotenv.2020.139793.

[4] Chen S D, Lan Y B, Zhou Z Y, Deng X L, Wang J. Research advances of the drift reducing technologies in application of agricultural aviation spraying. Int J Agric & Biol Eng, 2021; 14(5): 1–10.

[5] Law S E. Electrostatic pesticide spraying: concepts and practice. IEEE Transactions on Industry Applications, 1983; 19(2): 160–168.

[6] Ru Y, Zhou H P, Shu C R. Deposition evaluation of aerial electrostatic spraying system assembled in fixed-wing. Applied Engineering in Agriculture, 2014; 30(5): 751–757.

[7] Hao Z Y, Li X Z, Meng C, Yang W, Li M Z. Adaptive spraying decision system for plant protection unmanned aerial vehicle based on reinforcement learning. Int J Agric & Biol Eng, 2022; 15(4): 16–26.

[8] Khoshnevis A, Tsai S S H, Esmaeilzadeh E. Electric field induced

sheeting and breakup of dielectric liquid jets. Physics of Fluids, 2014; 26(1): 197–219.

[9] Ru Y, Jin L, Jia Z C, Bao R, Qian X D. Design and experiment on electrostatic spraying system for unmanned aerial vehicle. Transactions of the CSAE, 2015; 31(8): 42–47. (in Chinese)

[10] Lan Y B, Chen S D. Current status and trends of plant protection UAV and its spraying technology in China. International Journal of Precision Agricultural Aviation, 2018; 1(1): 1–9.

[11] Patel M K, Praveen B, Sahoo H K, Sahoo H K, Patel B, Kumar A, et al. An advance air-induced air-assisted electrostatic nozzle with enhanced performance. Computers and Electronics in Agriculture, 2017; 135: 280–288.

[12] Patel M K, Sahoo H K, Nayak M K, Kumar A, Kumar A. Electrostatic nozzle: New trends in agricultural pesticides spraying. National Conference on Emerging Fields in Engineering and Sciences (EFES-2015), 2015; pp.6–11.

[13] Law S E, Bowen S. Charging liquid spray by electrostatic induction. Transactions of the ASAE, 1966; 9(4): 501–506.

[14] Law S E, Thompson S A, Balachandran W. Electroclamping forces for controlling bulk particulate flow: charge relaxation effects. Journal of Electrostatics, 1996; 37(1-2): 79–93.

[15] Ru Y, Zhou H P, Jia Z C, Wu X W, Fan Q N. Design and application of electrostatic spraying system. Journal of Nanjing Forestry University (Natural Sciences Edition), 2011; 35(1): 91–94. (in Chinese)

[16] Fritz B K, Hoffmann W C, Martin D E, Thomson S J. Aerial application methods for increasing spray deposition on wheat heads. Applied Engineering in Agriculture, 2007; 23(6): 709–715.

[17] Inculet I I, Fischer J K. Electrostatic aerial spraying. IEEE Transactions on Industry Applications, 1989; 25(3): 558–562.

[18] Zhang Y L, Lan Y B, Bradley K, Xue X Y. Development of aerial electrostatic spraying systems in the United States and applications in China. Transactions of the CSAE, 2016; 32(10): 1–7. (in Chinese)

[19] Lan Y B, Zhang H Y, Wen S, Li S H. Analysis and experiment on atomization characteristics and spray deposition of electrostatic nozzle. Transactions of the CSAM, 2018; 49(4): 130–139. (in Chinese)

[20] Maski D, Durairaj D. Effects of charging voltage, application speed, target height, and orientation upon charged spray deposition on leaf abaxial and adaxial surfaces. Crop Protection, 2010; 29(2): 134–141.

[21] Maski D, Durairaj D. Effects of electrode voltage, liquid flow rate, and liquid properties on spray chargeability of an air-assisted electrostatic-induction spray-charging system. Journal of Electrostatics, 2010; 68(2): 152–158.

[22] Zhang H X, Ru Y. Experimental study on rotor airflow electrostatic atomization device. Journal of Chinese Agricultural Mechanization, 2016; 37(12): 57–62. (in Chinese)

[23] Liu D J, Gong Y, Wang G, Zhang X, Chen X. Development of centrifugal atomization technique in the field of plant protection machinery. Plant Diseases & Pests, 2017; 8(3): 39–42. (in Chinese)

[24] Liu J, Yu Q, Guo Q. Experimental investigation of liquid disintegration by rotary cups. Chemical Engineering Science, 2012; 73: 44–50.

[25] Craig I P, Hewitt A, Terry H. Rotary atomiser design requirements for optimum pesticide application efficiency. Crop Protection, 2014; 66: 34–39.

[26] Derksen R C, Zhu H, Ozkan H E, Hammond R B, Dorrance A E, Spongberg A L. Determining the influence of spray quality, nozzle type, spray volume, and air-assisted application strategies on deposition of pesticides in soybean canopy. Transactions of the ASABE, 2008; 51(5): 1529–1537.

[27] Bayat A, Bozdogan N Y. An air-assisted spinning disc nozzle and its performance on spray deposition and reduction of drift potential. Crop Protection, 2005; 24(11): 951–960.

[28] Lavers A. Pesticide application methods. Crop Protection, 1983; 2(1): 122–123.

[29] Zhou H Y, Chen H. Space distribution of electrical field generated by a uniformly charged ring. College Physics, 2004; 9: 32–34. (in Chinese)

[30] He Y J, Zhao B B, Yu Y C. Effect, comparison and analysis of pesticide electrostatic spraying and traditional spraying. Bulgarian Chemical Communications, 2016; 48(Special Issue D): 340–344.